

# First-principles calculation of the phonon spectrum of $\text{MgAl}_2\text{O}_4$ spinel

G. A. de Wijs,<sup>1</sup> C. M. Fang,<sup>2</sup> G. Kresse,<sup>3</sup> and G. de With<sup>2</sup>

<sup>1</sup>*Electronic Structure of Materials, Research Institute for Materials, Faculty of Sciences, Toernooiveld 1, NL-6525 ED Nijmegen, The Netherlands*

<sup>2</sup>*Laboratory of Solid State and Materials Chemistry, Eindhoven University of Technology, P.O. Box 513, NL-5600 MB Eindhoven, The Netherlands*

<sup>3</sup>*Institut für Materialphysik, Universität Wien, Sensengasse 8, A-1090 Wien, Austria*

(Received 26 July 2001; published 20 February 2002)

The phonon spectrum of a  $\text{MgAl}_2\text{O}_4$  spinel has been calculated from first principles using density-functional theory. The spinel was perfectly ordered with space group  $Fd\bar{3}m$ . The five Raman active and four infrared active modes allowed by symmetry are unambiguously identified. Agreement with available Raman, infrared, and inelastic neutron scattering data is good. The fifth Raman mode (missing in experiment) is located at  $570\text{ cm}^{-1}$ .

DOI: 10.1103/PhysRevB.65.094305

PACS number(s): 63.20.Dj, 78.30.Hv

## I. INTRODUCTION

Spinel  $\text{MgAl}_2\text{O}_4$  has been the subject of intense study for several reasons. This natural mineral is the archetype of many compounds that crystallize in the same structure.<sup>1,2</sup> It is the dominant component of the spinel phase in Earth's shallow mantle.<sup>1,3</sup> Moreover, it has a combination of several desirable properties such as a high melting temperature, high strength, resistance to chemical attack and ion bombardment at elevated temperatures, and low electrical loss.<sup>4</sup> Therefore the material has many applications, e.g., in refractory ceramics, as electrical dielectric and irradiation resistant material. In addition, it can be used as an envelope material in high-pressure discharge lamps, to replace quartz glass.<sup>5</sup> Other applications are in heterogeneous catalysis,<sup>6</sup> as humidity sensors<sup>7</sup> and ultrafiltration membranes.<sup>8</sup>

The crystal structure of  $\text{MgAl}_2\text{O}_4$  is cubic, fcc, with space group  $Fd\bar{3}m$  ( $O_h^7$ , No. 227 in the International Tables<sup>9</sup>).<sup>10,11</sup> Mg, Al, and O are at Wyckoff position  $8a$ ,  $16d$ , and  $32e$ , respectively. The structure is fully determined by the lattice constant  $a$  and the anion parameter  $x$  of the positions  $32e$ . The anions are on an approximate close-packed fcc lattice, with the Al and Mg cations at octahedral and tetrahedral interstitial positions, respectively. Spinel is highly prone to cation disorder: Some, in inverted spinel even all, Mg ions may exchange positions with Al ions. This problem is particularly severe in synthetic spinels. Natural spinels have less cation disorder.

The vibrational properties of spinel  $\text{MgAl}_2\text{O}_4$  have been studied with Raman<sup>12–16</sup> (R) and infrared (IR) spectroscopy.<sup>12,15,17–22</sup> To our knowledge, only one study using inelastic neutron scattering is available.<sup>23</sup> Thus most experimental data is restricted to the vicinity of the  $\Gamma$  point of the Brillouin zone (BZ). Infrared studies have led to some controversy, as authors reported differing numbers of IR-active modes. Only four IR-active modes are allowed by symmetry. For Raman spectroscopy only four of the five allowed modes have been reported for natural spinel. The

occurrence of yet another mode has been demonstrated to result from cation disorder.<sup>16</sup>

In this paper we report first-principles calculations of the phonon spectrum of a  $\text{MgAl}_2\text{O}_4$  spinel, throughout the full BZ. The calculations unambiguously identify the positions of the Raman and IR-active modes, in the absence of any disorder. They may serve as a reference, and thus help to discriminate between those experimentally observed modes that are intrinsic to the lattice and those that arise from defects, such as cation disorder. Moreover, they should constitute a reference for approximate models of a spinel that are needed in the simulation of fracture experiments<sup>24</sup> and low-index complicated surfaces.

## II. COMPUTATIONAL DETAILS

Calculations were carried out with the first-principles molecular-dynamics program VASP (Vienna *ab initio* simulation program).<sup>25–27</sup> This program calculates the electronic structure and, via the Hellmann-Feynman theorem, the interatomic forces from first-principles.

The phonon spectrum has been calculated with the method of Ref. 28. In this direct method, the interatomic force-constant matrix is derived from a set of calculations on a periodically repeated supercell that is a multiple of several unit cells. As a starting point, all atoms are put into their equilibrium positions. Then an atom is slightly displaced, and the forces on all atoms in the cell are calculated. These forces are proportional to the interatomic force constants times the displacement. By considering all symmetry-inequivalent displacements, the full force-constant matrix can be obtained. It is truncated due to the finite size of the supercell. However, it rapidly decays to zero with increasing interatomic separation. The phonon frequencies as a function of the  $\mathbf{q}$  vector are obtained by a straightforward diagonalization of the dynamical matrix.<sup>29</sup>

The above method is only correct for the analytical part of the dynamical matrix, as it imposes a translational symmetry on the supercell. The nonanalytical part describes the effect

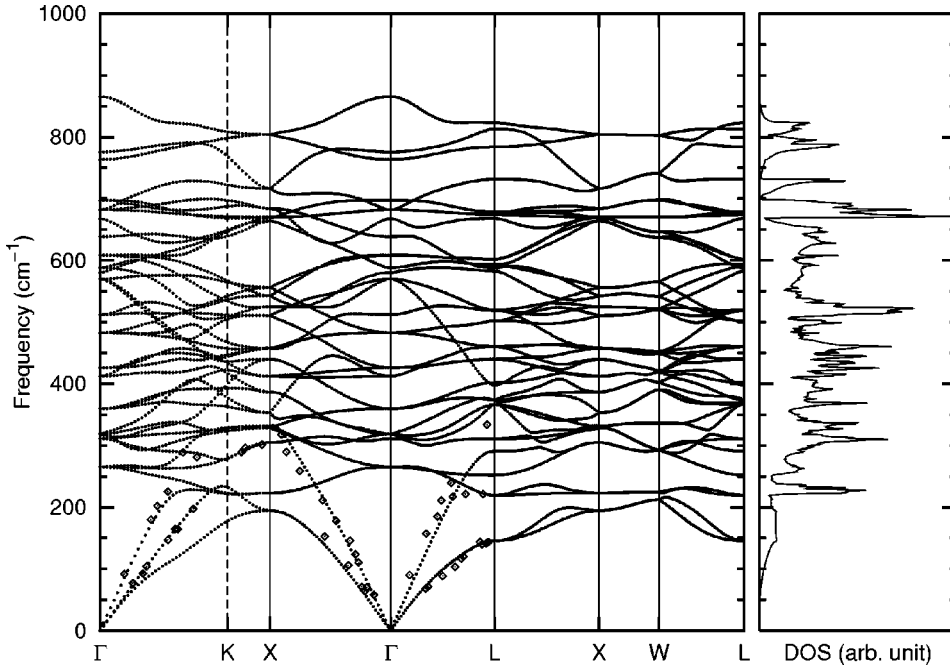


FIG. 1. Calculated phonon-dispersion curves (left) and density of states (right) of a  $\text{MgAl}_2\text{O}_4$  spinel. Experimental results by Thompson and Grimes (diamonds) (Ref. 23).

of the macroscopic electrostatic field that arises for certain LO modes in the long-wavelength limit ( $\mathbf{q} \rightarrow \Gamma$ ). Thus it lifts the LO-TO degeneracy of these modes. The field is a consequence of the incomplete screening in semiconductors and insulators, and is reflected by the Born effective charges carried by the ions. We account for this nonanalytical part following the method outlined in Ref. 30: Due to the neglect of the nonanalytical contribution, the interplanar force constants do not tend to zero for large interplanar separation, but they converge to finite, nonzero values.<sup>31</sup> From these, the effect of the nonanalytical part can be calculated. For more details we refer to Refs. 30 and 32.

The supercell contains eight conventional unit cells in a  $2 \times 2 \times 2$  arrangement. Thus it contains 448 atoms. For each atomic species only one displacement ( $0.04 \text{ \AA}$ ) was necessary.

After optimization of the oxygen parameter  $x$ , very small residual forces remained ( $\sim 0.001 \text{ eV/\AA}$ ). For a phonon calculation using a conventional unit cell, these have a negligible effect on the accuracy of the phonon frequencies. However, in the  $2 \times 2 \times 2$  cell all eight residual forces (of the eight conventional cells) are folded back, and the error is amplified eight times, having a detrimental effect on the highest Raman-active mode at  $\Gamma$ . By subtracting the spurious forces in the equilibrium configuration from those obtained with the atoms displaced we correct for this effect in leading order. This restores the accuracy of the calculation.

The longitudinal interplanar force constants are also obtained from the  $2 \times 2 \times 2$  cell. It is already quite long ( $16.06 \text{ \AA}$ ). We checked the resulting LO-TO splitting with a longer  $3 \times 1 \times 1$  cell, and found only minor deviations. Moreover, with this longer cell we could check (for the  $\Gamma$ -X direction) that the phonon spectrum is well converged with a  $2 \times 2 \times 2$  supercell, i.e., that the analytical part is sufficiently short range.

The electronic wave functions were sampled only at the  $\Gamma$

point of the Brillouin zone of the supercell. Using a smaller  $1 \times 1 \times 1$  cell,  $\mathbf{k}$ -point convergence was checked. Norm-conserving pseudopotentials were used for Mg and Al (Ref. 33), and an ultrasoft pseudopotential was used for O.<sup>34,35</sup> The kinetic-energy cutoff on the wave functions was 495 eV (36 Ry). For the (augmentation) charge a cutoff of 928 eV (68 Ry) was used. Convergence tests were carried out in a  $1 \times 1 \times 1$  cell with cutoffs up to 900 and 1600 eV respectively. The frequencies of the modes at  $\Gamma$  are accurate within two wave numbers on average. The nonlocal projection of the pseudopotentials were carried out in real space.<sup>36</sup> Calculations were carried out in the local-density approximation (LDA).<sup>37</sup>

TABLE I. Frequencies  $f$  of the optical modes of the spinel at the  $\Gamma$  point of the primitive unit cell. For the infrared active species, the frequencies of the LO phonon are between brackets.

| Species             | $f \text{ (cm}^{-1}\text{)}$ |
|---------------------|------------------------------|
| $T_{2u}$            | 265                          |
| $T_{1u}(\text{IR})$ | 311 (319)                    |
| $T_{2g}(\text{R})$  | 319                          |
| $T_{1g}$            | 360                          |
| $E_u$               | 412                          |
| $E_g(\text{R})$     | 426                          |
| $T_{2u}$            | 483                          |
| $T_{1u}(\text{IR})$ | 512 (580)                    |
| $T_{2g}(\text{R})$  | 570                          |
| $T_{1u}(\text{IR})$ | 588 (638)                    |
| $E_u$               | 608                          |
| $A_{2u}$            | 668                          |
| $T_{2g}(\text{R})$  | 682                          |
| $T_{1u}(\text{IR})$ | 698 (866)                    |
| $A_{2u}$            | 763                          |
| $A_{1g}(\text{R})$  | 776                          |

TABLE II. Frequencies of the optical modes of the spinel at the  $\Gamma$  point of the primitive unit cell. Experimental Raman frequencies are from O'Horo *et al.* (Ref. 12), Mal ezieux and Piriou (Ref. 14), Chopelas and Hofmeister (Ref. 15), and Cynn *et al.* (Ref. 16). All frequencies are in  $\text{cm}^{-1}$ .

| Species  | Calculated | O'Horo <i>et al.</i> | Mal ezieux and Piriou | Chopelas and Hofmeister | Cynn <i>et al.</i> |
|----------|------------|----------------------|-----------------------|-------------------------|--------------------|
| $T_{2g}$ | 319        | 311                  | 311                   | 312                     | 311                |
| $E_g$    | 426        | 410                  | 408                   | 407                     | 409                |
| $T_{2g}$ |            | 492                  |                       |                         |                    |
| $T_{2g}$ | 570        |                      |                       |                         |                    |
| $T_{2g}$ | 682        | 671                  | 669                   | 666                     | 670                |
| $A_{1g}$ |            | 727                  |                       |                         | (727)              |
| $A_{1g}$ | 776        | 772                  | 770                   | 767                     | 770                |

### III. RESULTS

First the crystal structure was optimized. After minimization, we obtained  $a=8.030 \text{ \AA}$  and  $x=0.3891$ .<sup>38</sup> In natural spinel, which has less cation disorder than synthetic spinel,  $a=8.0989 \text{ \AA}$  and  $x=0.387$ .<sup>39</sup> A slight underestimation of the lattice constant is not unusual in LDA calculations. In all phonon calculations the calculated values of  $a$  and  $x$  were used.

The calculated phonon spectrum along a few high-symmetry directions in the BZ and the phonon density of states (PDOS) are shown in Fig. 1. The latter was calculated by linear tetrahedron integration of the phonon frequencies calculated on a  $20 \times 20 \times 20$   $\mathbf{q}$ -point mesh. The PDOS and the spectrum have a very complicated structure, as there are 42 branches. Near the upper end of the frequency scale the PDOS develops a few prominent, almost isolated, peaks.

Most experimental data on the frequencies comes from infrared and Raman experiments. These experiments only provide information on the long-wavelength limit. In Table I we list all the calculated frequencies at the  $\Gamma$  point. They have been classified following the factor group analysis by White and DeAngelis.<sup>40</sup>

The crystal symmetry allows for five Raman-active modes. In Table II results, of the Raman experiments by O'Horo *et al.*,<sup>12</sup> Mal ezieux and Piriou,<sup>14</sup> Chopelas and Hofmeister,<sup>15</sup> and Cynn *et al.*<sup>16</sup> are listed. O'Horo *et al.* used a synthetic spinel whereas the others used natural spinel. The calculated frequencies at 319, 426, 682, and 776  $\text{cm}^{-1}$  agree with the experimental values within 1–5%. We obtain the fifth mode at 570  $\text{cm}^{-1}$ . None of the experiments listed in Table II reported a mode near this frequency. O'Horo *et al.* (synthetic spinel) did find a fifth band at 492  $\text{cm}^{-1}$ , which is

rather weak. However, the discrepancy with 570  $\text{cm}^{-1}$  is too large. So we expect that the 492- $\text{cm}^{-1}$  band is another mode, characteristic of a synthetic spinel. Its occurrence is probably related to cation disorder, which is known to be much more abundant in synthetic spinel compared to natural spinel. The fifth mode (of natural spinel) should be close to the calculated value of 570  $\text{cm}^{-1}$ . Its oscillator strength is presumably so small that it has not yet been observed. We note that Fraas *et al.*,<sup>13</sup> who studied many different spinel samples (synthetic and natural) did observe weak modes at 555 and 600  $\text{cm}^{-1}$ .

We do not observe a mode near 727  $\text{cm}^{-1}$ , which Cynn *et al.*<sup>16</sup> observed in natural spinel, but only after annealing. They conclude that it results from  $\text{AlO}_4$  tetrahedra, i.e., from cation disorder. Consistently, Mal ezieux and Piriou,<sup>14</sup> Chopelas and Hofmeister<sup>15</sup> and we do not observe this mode. To further test this assignment, calculations with an  $\text{AlO}_4$  tetrahedron were carried out. These are described in the Appendix. The  $\text{AlO}_4$  impurity is found to have two breathing modes, one of which is at 723  $\text{cm}^{-1}$ , i.e., close to 727  $\text{cm}^{-1}$ .

The experimental IR data are more controversial than the Raman data. Symmetry allows for four  $T_{1u}$  modes. The induced macroscopic electrical field lifts the threefold degeneracy, so that each IR active  $T_{1u}$  mode splits into a twofold degenerate TO level and a single LO mode.

Table III lists data from several IR experiments. The calculated frequencies are in very good agreement with those by Preudhomme and Tarte<sup>19</sup> on natural spinel.

Agreement with the data of O'Horo *et al.*<sup>12</sup> on a synthetic spinel is worse; in particular the 428- $\text{cm}^{-1}$  mode differs strongly from the calculated 512  $\text{cm}^{-1}$ . Grimes *et al.*<sup>22</sup> have reanalyzed the reflectivity data of O'Horo *et al.* and con-

TABLE III. Frequencies of the optical modes of the spinel at the  $\Gamma$  point of the primitive unit cell, listed as TO (LO). Experimental frequencies are from Preudhomme and Tarte (Ref. 19), O'Horo *et al.* (Ref. 12), and Chopelas and Hofmeister (Ref. 15). Frequencies by Grimes *et al.* are also listed.<sup>22</sup> All frequencies are in  $\text{cm}^{-1}$ .

| Calculated | Preudhomme and Tarte | O'Horo <i>et al.</i> | Grimes <i>et al.</i> | Chopelas and Hofmeister |
|------------|----------------------|----------------------|----------------------|-------------------------|
| 311 (319)  | 309                  | 305                  | 305 (305)            | 304 (312)               |
| 512 (580)  | 522                  | 428                  | 485                  | 476 (610)               |
| 588 (638)  | 580                  | 485                  | (630)                | 578 (575)               |
| 698 (866)  | 688                  | 670                  | 670 (855)            | 676 (868)               |

cluded that there are two transverse modes, at 485 and 670  $\text{cm}^{-1}$ , with the corresponding longitudinal modes at 630 and 855  $\text{cm}^{-1}$ . Moreover, they suggested that a third mode with very small splitting may be present near 305  $\text{cm}^{-1}$ . Thus they lacked one (split)  $T_{1u}$  mode. They found support for their interpretation (i.e., only three modes) from a good agreement with the Lyddane-Sachs-Teller (LST) rule,

$$\frac{\epsilon(0)}{\epsilon(\infty)} = \prod_i \frac{\omega_i^2(\text{LO})}{\omega_i^2(\text{TO})},$$

where  $\epsilon$  denotes the dielectric function. For the left-hand side they obtain 2.84, and for the right hand side 2.75. We try to make contact with their interpretation: The TO modes at 485 and 670  $\text{cm}^{-1}$  can be assigned to the calculated modes at 512 and 698  $\text{cm}^{-1}$ . The LO modes at 630 and 855  $\text{cm}^{-1}$  can be identified with the modes at 638 and 866  $\text{cm}^{-1}$ . Thus the maximum discrepancy with experiment is 5.5%, only slightly larger than usual for density-functional calculations. The calculated mode at 311 (319)  $\text{cm}^{-1}$  confirms the possibility of a mode near 305  $\text{cm}^{-1}$ . Thus we have not assigned the calculated TO mode at 588  $\text{cm}^{-1}$  and the calculated LO mode at 580  $\text{cm}^{-1}$ . Note that these frequencies almost coincide, so that inclusion of these two modes in the LST rule hardly affects the right-hand side. Indeed, the real part of the dielectric function, as plotted by Grimes *et al.*, exhibits a wiggle just near 600  $\text{cm}^{-1}$ . We speculate that this wiggle is caused by the close proximity of the 580- and 588- $\text{cm}^{-1}$  bands.

Note that the calculated frequencies give 2.45 for the right-hand side of the LST. The agreement is reasonable, as errors in the frequencies are amplified by the power. Several explanations for this discrepancy are conceivable, such as the approximation made by density-functional theory and the LST rule itself being only an approximation.

Comparison with the data by Chopelas and Hofmeister<sup>15</sup> gives yet another picture. These authors carried out reflectivity measurements on a single-crystal, highly ordered, natural spinel. Therefore, their results should be most accurate. They resolved the complete number of symmetry-allowed modes. Indeed the modes not observed by Grimes *et al.* are present in their data, but they are very weak. Their frequencies give 2.82 for the right-hand side of the LST, in very close agreement with the left-hand side (2.84). For six of the eight frequencies, our data and that of Chopelas and Hofmeister agree within 3%. Larger discrepancies exist for the pairs 512 and 476 (7%) and 638 and 610 (5%).<sup>41</sup>

Away from the  $\Gamma$  point of the BZ, the experimental data are much less abundant. Thompson and Grimes (Ref. 23) carried out inelastic neutron-scattering experiments on a synthetic spinel, and obtained part of the dispersion curves. Comparison is made in Fig. 1. Agreement is fairly good for  $\Gamma$ - $(K)$ - $X$ - $\Gamma$  and the lower part of the acoustic branches for  $\Gamma$ - $L$ . A small disagreement is apparent for the higher part (200  $\text{cm}^{-1}$  and above) along  $\Gamma$ - $L$ . Moreover, the experimental point near  $L$  at 330  $\text{cm}^{-1}$  is not on a calculated branch. We think that these small differences can be ac-

counted for by the substantial cation inversion in the synthetic spinel used by Thompson and Grimes in their measurements.<sup>23</sup>

#### IV. CONCLUSIONS

In summary, the phonon spectrum of  $\text{MgAl}_2\text{O}_4$  spinel has been calculated from first principles. Good agreement with experiment is obtained for the four experimentally clearly observed Raman-active modes. In general, the calculated frequencies are slightly larger than the experimental frequencies. The fifth calculated mode at 570  $\text{cm}^{-1}$  cannot be assigned to the 492- $\text{cm}^{-1}$  band observed for synthetic spinel. The oscillator strength for the 570- $\text{cm}^{-1}$  band is presumably very small. We speculate that the 492- $\text{cm}^{-1}$  band arises from disorder. The calculations are in reasonable agreement with experiments concerning the observed infrared active modes.

The phonons were calculated for the optimized LDA volume, which is approximately 1% smaller than the experimental volume. This could have a small effect on the frequencies calculated, i.e., could possibly account for the small overestimation.

#### ACKNOWLEDGMENTS

This work is part of the research program of the Stichting voor Fundamenteel Onderzoek der Materie (FOM) with financial support from the Nederlandse Organisatie voor Wetenschappelijk Onderzoek (NWO).

#### APPENDIX: AN $\text{AlO}_4$ TETRAHEDRON

An  $\text{AlO}_4$  tetrahedron was modeled in a  $1 \times 1 \times 1$  supercell (56 atoms). In a first attempt, the  $\text{AlO}_4$  was obtained by the exchange of an Al atom and a Mg atom. Care was taken to have the interchanged atoms as far apart as possible. However, the modes of the  $\text{AlO}_4$  tetrahedron were still strongly perturbed by the presence of the Mg atom at the Al site, and this attempt was abandoned. Instead, we only changed the identity of one Mg ion into an Al. Thus the composition of the cell deviates from stoichiometry. In order to preserve the gap, we fixed the number of electrons, such as to exactly fill the oxygen  $2p$  band ( $\text{Mg}_7^{2+} \text{Al}_{17}^{3+} \text{O}_{32}^{2-}$ ). To keep the cell neutral a uniform, negative background charge was added. The lattice constant was fixed at the bulk value and the structure was relaxed until no nonzero forces remained. The Al-O distance in the tetrahedron is 1.79 Å. For this structure the phonons at  $\Gamma$  were calculated. The results should be interpreted with care, as the Al atom in the tetrahedron is separated from its nearest periodic images by a distance of only 8.03 Å. It is not unlikely that in reality the relaxations of atomic shells around the Al ion extend to a larger distance than the distance (4 Å) that can be properly described in the  $1 \times 1 \times 1$  cell. Calculations on a larger cell are therefore desirable. However, due to the low symmetry they require a prohibitively large computational effort as many more displacements than the three required for the ideal crystal are necessary.

We find two modes, at 723 and 757  $\text{cm}^{-1}$ , with the character of an  $\text{AlO}_4$  breathing motion (with a large amplitude). They differ in how the oscillating  $\text{AlO}_4$  couples with the vibrational motion of the surrounding lattice. The second coordination shell of the central Al atom consists of Mg, Al, and O atoms. For the 723- $\text{cm}^{-1}$  mode the Al atoms in this shell move outward when the oxygens of the tetrahedron move inward, whereas the oxygens from the second shell oscillate in phase with the oxygens of the tetrahedron. In contrast, for the 757- $\text{cm}^{-1}$  mode the oxygens from the second shell move opposite to the breathing motion of the oxy-

gens in the tetrahedron. For this mode the Al atoms from the second shell do hardly move.

The mode at 723  $\text{cm}^{-1}$  comes very close to the mode at 727  $\text{cm}^{-1}$  observed by Cynn *et al.*<sup>16</sup> and assigned by them to an  $\text{AlO}_4$  breathing motion. The close correspondence supports this assignment. The 757- $\text{cm}^{-1}$  mode, however, is not observed in experiment. Supposing its intensity is very weak, it might not be difficult to discern so close to the 770- $\text{cm}^{-1}$  peak of natural spinel. A calculation of the oscillator strengths of both modes would be desirable, but is beyond the scope of the present study.

- 
- <sup>1</sup>F. S. Galasso, *Structure and Properties of Inorganic Solids* (Pergamon, Oxford, 1970).
- <sup>2</sup>N. W. Grimes, *Phys. Technol.* **6**, 22 (1975); A. Zerr, G. Miede, G. Serghiou, M. Schwarz, E. Kroke, R. Riedel, H. Fuess, P. Kroll, and R. Boehler, *Nature (London)* **400**, 340 (1999); K. E. Sickafus and R. Hughes, *J. Am. Ceram. Soc.* **82**, 3277 (1999), and references therein.
- <sup>3</sup>E. G. Ravenstein, *Nature (London)* **44**, 423 (1891).
- <sup>4</sup>J. M. Leger, J. Haines, M. Schmidt, J. P. Petitot, A. S. Pereira, and J. A. H. daJornada, *Nature (London)* **383**, 401 (1996); W. Jones and L. J. Miles, *Proc. Br. Ceram. Soc.* **19**, 161 (1971).
- <sup>5</sup>R. J. Bratton, *J. Am. Ceram. Soc.* **57**, 283 (1974); A. Ghosh *et al.*, *J. Am. Ceram. Soc.* **74**, 1624 (1991).
- <sup>6</sup>A. Govindaraj, E. Flahaut, C. Laurent, A. Peigney, A. Rousset, and C. N. R. Rao, *J. Mater. Res.* **14**, 2567 (1999).
- <sup>7</sup>P. P. L. Regtien, *Sens. Actuators* **2**, 85 (1981/82); G. Gusmano, G. Montesperelli, E. Traversa, and G. Mattogno, *J. Am. Ceram. Soc.* **76**, 743 (1993).
- <sup>8</sup>A. Larbot, G. Philip, M. Persin, and L. Cot, *Key Eng. Mater.* **132-136**, 1719 (1997).
- <sup>9</sup>*International Tables for Crystallography* (Reidel, Dordrecht, 1983), Vol. A.
- <sup>10</sup>W. H. Bragg, *Philos. Mag.* **30**, 305 (1915).
- <sup>11</sup>S. Nishikawa, *Proc. Math. Phys. Soc. Tokyo* **8**, 199 (1915).
- <sup>12</sup>M. P. O'Horo, A. L. Frisillo, and W. B. White, *J. Phys. Chem. Solids* **34**, 23 (1973).
- <sup>13</sup>L. M. Fraas, J. E. Moore, and J. B. Salzberg, *J. Chem. Phys.* **58**, 3585 (1973).
- <sup>14</sup>J.-M. Malézieux and B. Piriou, *Bull. Mineral.* **111**, 649 (1988).
- <sup>15</sup>A. Chopelas and A. M. Hofmeister, *Phys. Chem. Miner.* **18**, 279 (1991).
- <sup>16</sup>H. Cynn, S. J. Sharma, T. F. Cooney, and M. Nicol, *Phys. Rev. B* **45**, 500 (1992).
- <sup>17</sup>S. Hafner and S. Laves, *Z. Kristallogr.* **115**, 321 (1961).
- <sup>18</sup>G. A. Slack, *Phys. Rev.* **134A**, 1268 (1964).
- <sup>19</sup>J. Preudhomme and P. Tarte, *Spectrochim. Acta, Part A* **27**, 1817 (1971).
- <sup>20</sup>N. W. Grimes and A. J. Collett, *Phys. Status Solidi B* **43**, 591 (1971).
- <sup>21</sup>M. E. Striefler, and S. I. Boldish, *J. Phys. C* **11**, L237 (1978).
- <sup>22</sup>N. W. Grimes, P. J. O'Connor, and P. Thompson, *J. Phys. C* **11**, L505 (1978).
- <sup>23</sup>P. Thompson and N. W. Grimes, *Solid State Commun.* **25**, 609 (1978).
- <sup>24</sup>B. Lawn, *Fracture of Brittle Solids* (Cambridge University Press, Cambridge, 1993); T. E. Mitchell, L. Hwang, and A. H. Heuer, *J. Mater. Sci.* **11**, 264 (1976).
- <sup>25</sup>G. Kresse and J. Hafner, *Phys. Rev. B* **47**, 558 (1993); **49**, 14251 (1994).
- <sup>26</sup>G. Kresse and J. Furthmüller, *Comput. Mater. Sci.* **6**, 15 (1996).
- <sup>27</sup>G. Kresse and J. Furthmüller, *Phys. Rev. B* **54**, 11169 (1996).
- <sup>28</sup>G. Kresse, J. Furthmüller, and J. Hafner, *Europhys. Lett.* **32**, 729 (1995).
- <sup>29</sup>The Mg mass used was 24.305 a.m.u., corresponding to the natural mixture of the isotopes.
- <sup>30</sup>G. Kern, G. Kresse, and J. Hafner, *Phys. Rev. B* **59**, 8551 (1999).
- <sup>31</sup>This procedure yields a  $3 \times 3$  matrix of longitudinal interatomic force constants (all three species can experience forces due to displacements of planes with all three kinds of species). This information is overcomplete, as a knowledge of  $\epsilon_0$  and two of the Born charges completely determines all nine force constants. The  $3 \times 3$  matrix is symmetrized observing the constraints resulting from this requirement.
- <sup>32</sup>K. Kunc and R. M. Martin, *Phys. Rev. Lett.* **48**, 406 (1982).
- <sup>33</sup>A. M. Rappe, K. M. Rabe, E. Kaxiras, and J. D. Joannopoulos, *Phys. Rev. B* **41**, 1227 (1990).
- <sup>34</sup>D. Vanderbilt, *Phys. Rev. B* **41**, 7892 (1990).
- <sup>35</sup>G. Kresse and J. Hafner, *J. Phys.: Condens. Matter* **6**, 8245 (1994).
- <sup>36</sup>R. D. King-Smith, M. C. Payne, and J. S. Lin, *Phys. Rev. B* **44**, 13063 (1991); G. Kresse (unpublished).
- <sup>37</sup>D. M. Ceperley and B. J. Alder, *Phys. Rev. Lett.* **45**, 566 (1980); J. P. Perdew and A. Zunger, *Phys. Rev. B* **23**, 5048 (1981).
- <sup>38</sup>The cell choice 1 of *International Tables for Crystallography* (Ref. 9) was used.
- <sup>39</sup>E. J. Samuelson and O. Steinsvoll, *J. Phys. C* **8**, L427 (1975).
- <sup>40</sup>W. B. White and B. A. DeAngelis, *Spectrochim. Acta, Part A* **23**, 985 (1967).
- <sup>41</sup>The four LO modes are linear combinations of the four "missing" TO modes. It is possible, however, to assign each TO mode to a specific LO mode by slowly "switching on" the corrections for the LO-TO splitting, and noting which TO mode develops from which LO mode. Assignments in Table III have been made accordingly.